ISSN 2706-655X Vol.6, Issue 3: 109-116, DOI: 10.25236/IJFET.2024.060314

Robotic arm control system based on triple closed-loop BLDC

Zhuowei Xu[1,*], Chenghong Liu[1]

[1]School of Electrical and Information Engineering, Beihua University, Jilin, China
[*]Corresponding author: 2642093909@qq.com

Abstract: *This paper introduces the design and implementation of a three-closed-loop control system for brushless DC motors (BLDC) used in robotic arms. This paper introduces the design and implementation of a three-closed-loop control system for brushless DC motors (BLDC) used in robotic arms. The system integrates three closed-loop control strategies of speed, current and position, aiming to improve the dynamic response capability and steady-state accuracy of robotic arm operation. The framework of the system is built in the MATLAB/Simulink environment. The speed and current loop are adjusted through the PI controller, and the displacement sensor is used to accurately obtain the position information of each joint of the robotic arm. Combined with power electronic switching technology, this system achieves precise control of the BLDC motor in the robotic arm. Simulation experimental results show that the proposed three-closed-loop control system can effectively suppress external disturbances and significantly. In addition, the system also demonstrated excellent adaptability and stability under conditions of robot arm startup and load changes, proving that the system can be controlled by the BLDC motor in the robotic arm.*

Keywords: *brushless direct current motor (BLDC); three closed-loop control; robotic arm; PI controller; steady state accuracy*

1. Introduction

With the rapid development of industrial automation technology, robotic arms have become an integral part of modern manufacturing and automation. Their high degree of flexibility and precise control capability make robotic arms particularly important in performing complex tasks. However, with the increasing requirements for productivity and operational accuracy, the traditional dual closed-loop control system gradually exposes its limitations in terms of high accuracy and adaptability to complex environments. Especially in the face of model uncertainty and external disturbances, traditional control systems are often difficult to maintain efficient and stable performance.

Against this background, the concept of triple-closed-loop control system emerged, which not only optimises the dynamic response characteristics but also significantly improves the robustness of the system by introducing current closure as the third control dimension. Compared with the existing double-closed-loop system, the triple-closed-loop control system shows obvious advantages in terms of accuracy, stability, and adaptability to complex operating environments. In addition, the three-closed-loop system's resistance to external disturbances and adaptability under different load conditions are also significantly improved, which is of great practical significance to meet the increased performance requirements of modern industry for robotic arms[1]. This is of great practical significance to meet the improved performance requirements of modern industry.

The aim of this paper is to design and implement a robotic arm control system based on a three-closed-loop control strategy for a brushless DC motor (BLDC) drive. Through an in-depth analysis of the interaction mechanisms of the three closed loops of velocity, current and position, we propose a novel control scheme aiming to further enhance the dynamic responsiveness and steady-state accuracy of the robotic arm operation. The objective of this study is to verify the effectiveness of the three-closed-loop control system in improving the performance of the robotic arm through theoretical analyses and simulation experiments, and to explore its potential application in the field of high-precision mechanical operation.

ISSN 2706-655X Vol.6, Issue 3: 109-116, DOI: 10.25236/IJFET.2024.060314

2. System working structure

In the architecture of a modern robotic arm control system, the system usually consists of several core components, including an upper computer, a communication module, a control module, a drive module, a mechanical actuator unit (including a motor and its deceleration mechanism), and a position sensor. For the above components as shown in Figure 1, this study proposes a novel control module design, which utilises the fusion of a digital signal processor DSP28335 and a field-programmable logic gate array (FPGA), and achieves high-speed data communication between the two through the DSP28335's external interface XINT[2]. The strategy is adopted to improve the overall performance of the system, ensure real-time control, and reduce power consumption.

In this system, the DSP28335 takes on the responsibilities of general-purpose control logic and data processing, while the FPGA focuses on real-time signal processing and accelerated execution of algorithms. This synergy significantly improves the efficiency of data exchange and the response speed of the system. In addition, the selected external rotor-type brushless DC motor greatly adapts to the needs of the control system by virtue of its high torque density, excellent low-speed operation characteristics, low vibration noise and excellent heat dissipation capability. In the operation flow of the system, the host computer firstly gives commands to the control module through the communication module, and then the DSP28335 conducts high-speed data interaction with the FPGA through the XINTF, processes the received commands and generates the corresponding drive signals, which are then transmitted to the drive module to drive the motor. At the same time, the position sensor monitors and records the position information of the robotic arm in real time, which is processed by the FPGA and fed back to the DSP28335, based on which the DSP28335 compares and analyses the feedback data with the preset values, and adjusts the motor control commands to ensure that the robotic arm can accurately carry out the established operation tasks[3] . The design and implementation of such a system significantly enhances the overall performance and operational accuracy of the robotic arm control system by providing accurate data processing and rapid instruction feedback.

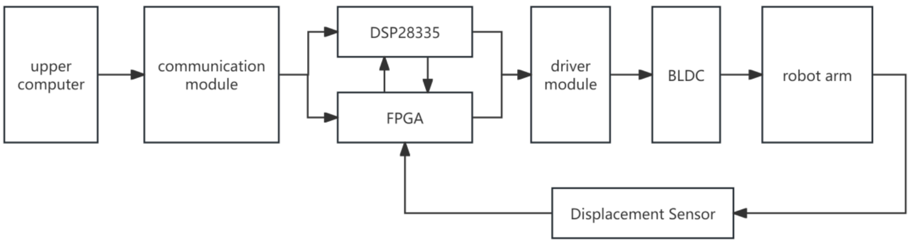

Figure 1: System framework diagram

3. Establishment of mathematical model for motor drive of robotic arm

When driving a robotic arm, it is first necessary to determine the angle or angular velocity of the arm, noted as θ_d or $\dot{\theta}_d$. Based on the difference between the actual arm angle or angular velocity and the control target, the error is calculated as $e = \theta_d - \theta$ or $e = \dot{\theta}_d - \dot{\theta}$. The duty cycle of the PWM signal is then adjusted by the PI controller according to the error signal[4]. to adjust the output torque of the motor.

When controlling BLDC (Brushless DC) motors, PI (Proportional-Integral) control is widely used to regulate the speed, current and position of the motor. Compared to PID (Proportional-Integral-Derivative) control, PI control has the advantages of simplicity, stability, and insensitivity to noise. Especially in the case of higher requirements for simplicity and stability, or system environment noise, PI control becomes a more suitable choice, more adaptable to the needs of the mass motor market. The output of the PI controller consists of only proportional and integral terms, and does not contain differential terms. The output formula is:

$$u(t) = K_p e(t) + K_i \int_0^t e(\tau)\, d\tau \tag{1}$$

Eq:$u(t)$ is the output of the controller;$e(t)$ is the error between the reference signal and the feedback signal;K_p is the proportional gain parameter;K_i is the integral gain parameter;$K_i \int_0^t e(\tau)\, d\tau$ is the integral of the error signal.

ISSN 2706-655X Vol.6, Issue 3: 109-116, DOI: 10.25236/IJFET.2024.060314

In practice, the PI control algorithms in the K_p and K_i are often tuned by system engineers based on experiments and information. Determining the appropriate values of these two parameters is a challenge and usually requires extensive experiments and literature research. Only through such efforts can accurate and stable control of motor operation be achieved.

According to the output of the controller$u(t)$, the duty cycle of the generated PWM signal$D$ which is usually achieved through a proportional relationship:

$$D = D_{min} + \frac{u(t)}{u_{max}} \times (D_{max} - D_{min}) \tag{2}$$

Of these, the D_{min} and D_{max} are the minimum and maximum duty cycles of the pwm signal, and u_{max} is the maximum value of the controller output.

The generated PWM signal is then sent to the motor's drive circuit to control the motor's output torque. According to the output torque of the motor, the robotic arm moves according to its dynamic equation to achieve proximity to the control target[5] .

By this method, the torque mode PWM is combined with the dynamic equations of the robotic arm to achieve the control of the robotic arm motion, and the controller adjusts the duty cycle of the PWM signal according to the difference between the actual state of the robotic arm and the target state. For the three-item four-pole BLDC modelling, it is assumed that the armature windings of the motor are uniformly and continuously distributed on the stator surface; the three-phase windings have perfect symmetry and the air-gap magnetic field is in the form of a trapezoidal waveform; eddy currents and hysteresis losses are not accounted for; the magnetic circuit is perfectly linear and there is no saturation effect; no friction between the mechanical parts exists; and the load is constant at 2.5 Nm;

The three armature winding voltages are:

$$V_a = \frac{2}{\sqrt{3}} \times D \times V_{max} \times \sin\theta_a \tag{3}$$

$$V_b = \frac{2}{\sqrt{3}} \times D \times V_{max} \times (\sin\theta_b - \tfrac{2}{3}\pi) \tag{4}$$

$$V_c = \frac{2}{\sqrt{3}} \times D \times V_{max} \times (\sin\theta_c + \tfrac{2}{3}\pi) \tag{5}$$

$$\begin{bmatrix} V_a \\ V_b \\ V_c \end{bmatrix} = \begin{bmatrix} R_a & 0 & 0 \\ 0 & R_b & 0 \\ 0 & 0 & R_c \end{bmatrix} \begin{bmatrix} I_a \\ I_b \\ I_c \end{bmatrix} + \begin{bmatrix} (L-M) & 0 & 0 \\ 0 & (L-M) & 0 \\ 0 & 0 & (L-M) \end{bmatrix} \begin{bmatrix} \frac{dI_a}{dt} \\ \frac{dI_b}{dt} \\ \frac{dI_c}{dt} \end{bmatrix} + \begin{bmatrix} e_a \\ e_b \\ e_c \end{bmatrix} \tag{6}$$

In the formula,V_a, V_b, V_c denote the phase a, b , c respectively.I_a , andI_b andI_c denote the currents in phases a and b , and c respectively, $\theta_a, \theta_b, \theta_c$are the phases of the corresponding pwm signals of phases a, b, c . e_a, e_b, e_c denote the reverse electromotive force of phases a, b, c , respectively.$\frac{dI_a}{dt}, \frac{dI_b}{dt}, \frac{dI_c}{dt}$denote the derivatives of the currents of phases respectively,with respect to time, i.e., the transformation rate of the current.

The phase difference between the reaction potential and the rotor position for each phase is 120° and there is a specific phase relationship between the reaction potential and the rotor position.

The instantaneous three-opposite electric potential is:

$$e_a = K_w \int(\theta_e)\,\omega \tag{7}$$

$$e_b = K_w \int(\theta_e - \frac{2\pi}{3})\,\omega \tag{8}$$

$$e_a = K_w \int(\theta_e + \frac{2\pi}{3})\,\omega \tag{9}$$

$K_w$is the coefficient of the reverse electromotive force of one phase;θ_e is the electrical angle of the rotor;ω is the rotor angular velocity .

Rotor mechanical angle θ_m and electrical angleθ_e relationship:

$$\theta_e = \frac{P}{2}\theta_m \tag{10}$$

where P is the number of rotor poles.

ISSN 2706-655X Vol.6, Issue 3: 109-116, DOI: 10.25236/IJFET.2024.060314

Therefore, the electromagnetic torque output from the motor is:

$$T_e = \frac{e_a i_a + e_b i_b + e_c i_c}{\omega} \tag{11}$$

The equation of motion of the motor is:

$$T_e - T_1 = J\frac{d\omega}{dt} + B\omega \tag{12}$$

T_1 is the load torque, and J is the moment of inertia, and B is the friction coefficient. According to the torque output from the motor, the robotic arm moves according to its dynamic equations to achieve proximity to the control target[6] .

4. Three Closed-loop Control Strategy for BLDC Motors

The three-closed-loop control system for brushless DC motors utilises position feedback, speed feedback and current feedback control loops to achieve precise regulation of the motor, as shown in Figure 2. These control loops interact with each other to jointly regulate the motor's operating state to ensure stable and efficient operation under various operating conditions.

In the system, the position feedback control loop is located at the outermost level. It is based on the set target position θ_d and the actual measured positionθ_d. It calculates the position error $\Delta\theta$ which is then processed by the proportional-integral (PI) regulation algorithm and the regulated output is passed to the speed feedback control loop.

The velocity feedback control loop receives the output of the position feedback control loop and measures the actual speed of the motorω and calculates the speed error $\Delta\omega$. This error is also processed by the PI regulation algorithm. This error is also processed by the PI regulation algorithm and is limited and fed into the current feedback control loop.

The current feedback control loop is the innermost control loop in the system. It receives the output of the speed feedback control loop and measures the current in each phase of the motor winding to calculate the current error. This error is processed by the PI regulation algorithm, and then limited and fed to the PWM pulse width regulator.[7] The PWM pulse width regulator.

Finally, the PWM pulse width regulator receives the output signal from the current feedback control loop and regulates the voltage of each phase winding of the DC brushless motor by driving the full-bridge inverter circuit, thus realising precise control of the motor.

This three-closed-loop control system not only achieves the goals of speed regulation and speed stabilisation, but also significantly improves the dynamic response and static performance of the system, enabling the motor to operate stably and efficiently under various operating conditions.

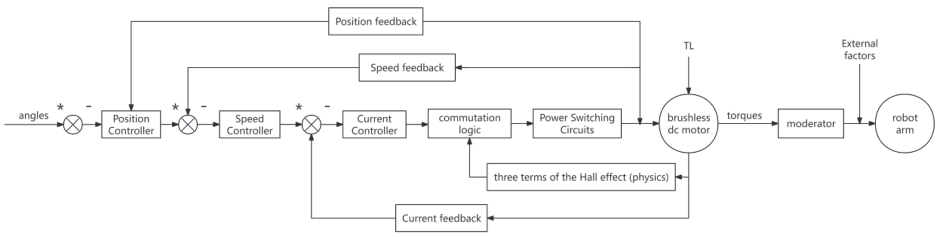

Figure 2: System Architecture Framework Diagram

5. Simulation Model of BLDC

In this paper, the simulation model is constructed by matlab/simulink as shown in Figure 3. The innermost loop is the current loop, which uses hysteresis loop regulation to respond to rapid changes and resist disturbances caused by voltage fluctuations. The hysteresis loop regulator is chosen for its simple working principle and fast response speed, which can resist the disturbance caused by voltage fluctuation in time. The intermediate loop is the speed loop, which uses PI (Proportional-Integral) control to provide effective disturbance suppression for load variations.[8] It uses PI (proportional-integral) control to provide effective interference suppression of load changes. When the controller reaches saturation, its saturation nonlinear characteristic kicks in and the amplitude limit of the output is constrained by the

ISSN 2706-655X Vol.6, Issue 3: 109-116, DOI: 10.25236/IJFET.2024.060314

maximum current allowed. The outermost loop is the position loop, which is responsible for accurately controlling the position of the motor and ensuring that the mechanical motion meets the predefined position target[9].

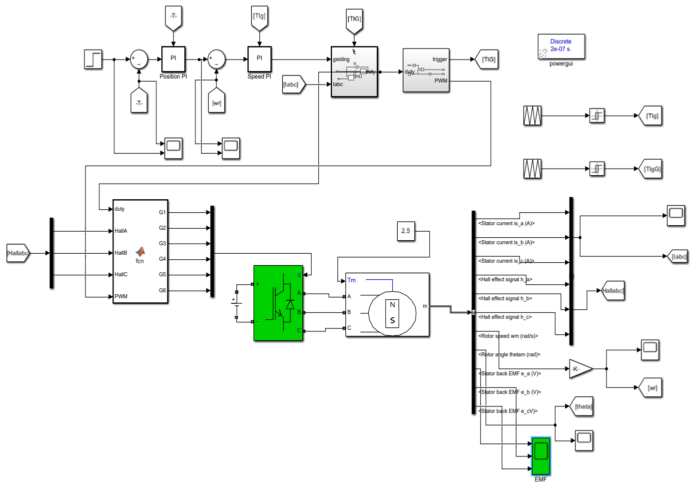

Figure 3: System simulation framework

The construction of commutation logic circuit module 1 and its logic function are demonstrated in Figure 4 and Table 1. The construction of module 2 and its logic function are then demonstrated in Fig. 5 and Table 2. The output signals of the Hall sensor are labelled as ha, hb, hc, while the three opposite electromotive force signals are denoted as emf_a, emf_b, emf_c. Q1 to Q6 identify the on-state signals of the power switching tubes in the inverter bridge.

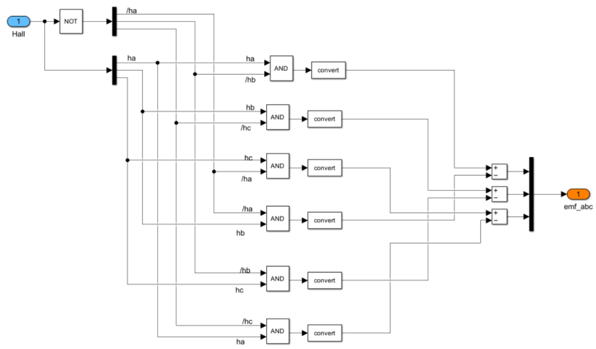

Figure 4: Logical framework of three-phase current commutation

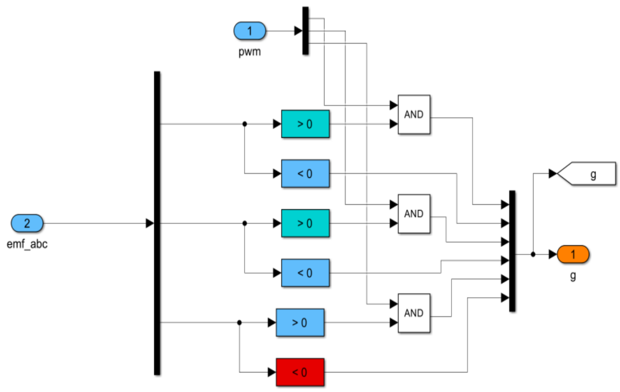

Figure 5: Logical framework diagram of three-phase inverter

ISSN 2706-655X Vol.6, Issue 3: 109-116, DOI: 10.25236/IJFET.2024.060314

Table 1: Logical functions of logical phase change module 1

ha	hb	hc	emf_a	emf_b	emf_c
0	0	0	0	0	0
0	0	1	0	-1	+1
0	1	0	-1	+1	0
0	1	1	-1	0	+1
1	0	0	+1	0	-1
1	0	1	+1	-1	0
1	1	0	0	+1	-1
1	1	1	0	0	0

Table 2: Logic functions of logic phase change module 2

ha	emf_b	emf_c	Q1	Q2	Q3	Q4	Q5	Q6
0	0	0	0	0	0	0	0	0
0	-1	+1	0	0	0	1	1	0
-1	+1	0	0	1	1	0	0	0
-1	0	+1	0	1	0	0	1	0
+1	0	-1	1	0	0	0	0	1
+1	-1	0	1	0	0	1	0	0
0	+1	-1	0	0	1	0	0	1
0	0	0	0	0	0	0	0	0

In this study, we use the MATLAB/Simulink environment to construct a simulation model of a permanent magnet brushless DC motor (BLDCM) control system, with parameters carefully tuned to reflect the actual motor performance: stator resistance of 0.0285 Ω, inductance of 7.5e-5H, torque constant of 0.078 Nm/A_peak, and a flat-topping region of the reverse electromotive force set at 120 degrees. The rotor inertia was set to 0.008 kg-m², viscous damping to 0.0004924 N-m-s/rad, pole-pair number 3, and sampling interval to 5 microseconds. During a 1.2 second simulation, the motor is started from no load to load application (3 N-m at 0.5 seconds) and its removal (at 0.9 seconds), capturing the speed, torque and current response, revealing the dynamic performance of the system.

6. Simulation Results

After in-depth system simulation analysis, the following system speed, torque, position, three-phase current and three-phase electromotive force simulation curves can be derived as shown in Figure 6-10.

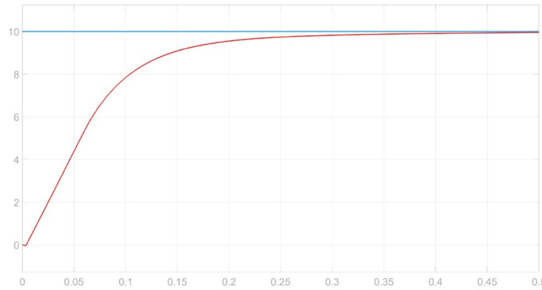

Figure 6: Speed Response Curve

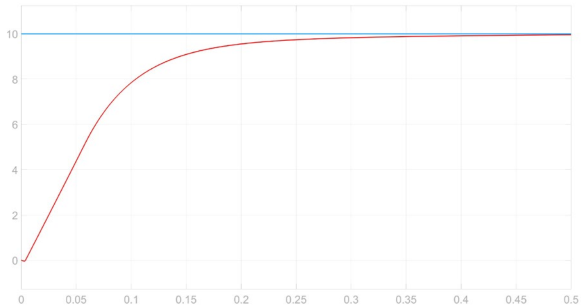

Figure 7: Torque response curve

ISSN 2706-655X Vol.6, Issue 3: 109-116, DOI: 10.25236/IJFET.2024.060314

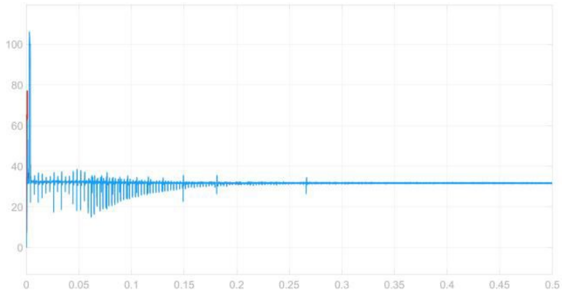

Figure 8: Current Response Curve

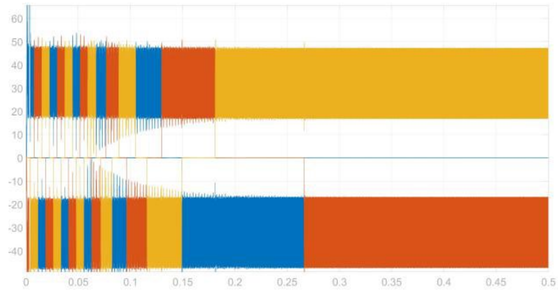

Figure 9: Three-phase current signal

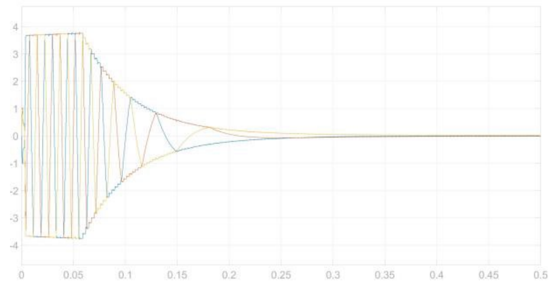

Figure 10: Three opposite electric potentials

As seen from the position response curves, the system exhibits a high degree of position tracking accuracy, and the consistency with the target trajectory indicates the effectiveness of the control strategy. However, the system overshoots when approaching the target set point, which suggests that careful parameterisation of the integral part of the Proportional-Integral (PI) controller is required to reduce the overshoot and improve the transient response of the system. For the speed response characteristics, the system quickly reaches and stabilises at the set speed value showing its fast and effective dynamic regulation, although the spikes in the initial transition of the speed response still need to be concerned, which may be related to the damping characteristics of the control system. The current response curves and the three-phase current signals reveal oscillations in the initial phase of the current control loop, which may be due to improper parameter settings in the control loop or to the inductive characteristics of the motor itself, pointing to the necessity of adjusting the PI control parameters in order to eliminate these oscillations. The analysis of the inverse electromotive force (EMF) waveform shows a certain degree of irregular fluctuations, which may suggest discontinuous changes in speed or inaccurate setting of the motor parameters, and which need to be carefully examined and parameter calibrated in order to ensure smooth operation of the motor[10] .

In summary, although the control system has good basic performance in terms of positioning accuracy and response speed, the parameter settings of the PI controller still need to be further optimised for the dynamic characteristics of the system and the operating environment to enhance the overall performance of the system and ensure its robustness under various operating conditions. These simulation results provide valuable guidance for the control system design and are important for achieving accurate and stable control.

ISSN 2706-655X Vol.6, Issue 3: 109-116, DOI: 10.25236/IJFET.2024.060314

7. Conclusion

In this study, a three-closed-loop control system of a brushless DC motor (BLDC) for a robotic arm was successfully designed and validated. Simulation results show that the triple-closed-loop control strategy integrating velocity, current and position feedback significantly improves the stability and efficiency of the robotic arm operation compared to the traditional single- and double-closed-loop control schemes. Under challenging conditions such as startup and sudden load changes, the system demonstrates excellent anti-disturbance performance and dynamic response capability. Combined with advanced power electronic switching technology and precise position sensing technology, the system not only optimises the dynamic performance of the robotic arm, but also improves its reliability in complex operating environments. In addition, by utilising the powerful functions of digital signal processor and field-programmable logic gate array, the real-time and energy-saving effects of the system are also significantly improved. Therefore, the proposed three-closed-loop control system is of great practical significance to meet the demand for high accuracy and stability in modern industrial applications, and provides new design ideas and solutions for the development of future robotic arm control systems.

References

[1] Cao Zipei,Annisa binti Jamali,Ren Yuan-Lin,et al. Analysis of BLDC torque pulsation suppression based on three closed-loop control system[J]. Journal of Lanzhou College of Arts and Sciences:Natural Science Edition, 2023, 37(4):68-73.

[2] Li Yaqian,Chen Qiang,Shi Huuhui et al. Scheduled-time repetitive learning control of a robotic arm [J/OL]. Control and Decision,1-8[2024-03-17].

[3] WU Pengfei,ZU Fengdan,CHEN Jingyuan et al. Design of multi-way brushless DC motor control system for flexible robotic arm based on FPGA[J]. Flight Control and Detection,2020,3(02):44-51.

[4] Chen Xuan,Hai Tao. Simulation analysis of BLDC motor for new photovoltaic lift system[J]. Heilongjiang Science and Technology Information, 2021(008):000.

[5] Zhang Kehan,Di Zhengfei,Liu Xiaoqiang et al. Simulation research on double closed-loop speed control system of brushless DC motor based on Matlab[J]. Micro motor,2015,48(02):44-48.

[6] Zheng Z. Design of a closed-loop control system for brushless DC motor without position sensor[D]. Nanjing University of Science and Technology, 2019.001403.

[7] Zhong Minghong. Research and design of sinusoidal wave drive power supply for brushless DC motor [D]. Jiangxi University of Science and Technology, 2014, DOI:10.7666/d.D570451.

[8] Wan Liguang. Simulation of dual closed-loop DC motor speed control system based on Matlab[J]. Marine Power Technology,2011,31(02):30-32.

[9] Ni Youyuan,Chen Hao,He Qiang,et al. A simple three-closed-loop control system for brushless DC motor without position sensor[J]. Journal of Electrical Machines and Control, 2017.

[10] Zhang L, Li Li. Modelling and simulation of brushless DC motor control system based on MATLAB [J]. Electromechanical Engineering Technology, 2010(4):4.